HHS Public Access

Author manuscript

Neuroimage. Author manuscript; available in PMC 2019 January 15.

Published in final edited form as:

Neuroimage. 2018 January 15; 165: 118–124. doi:10.1016/j.neuroimage.2017.10.009.

The Distribution of the Alpha7 Nicotinic Acetylcholine Receptor in Healthy Aging: An In Vivo Positron Emission Tomography Study with [^{18}F]ASEM

Jennifer M. Coughlin, M.D.[a,b,*], **Yong Du, Ph.D.**[b,*], **Hailey B. Rosenthal, B.A.**[b], **Stephanie Slania, B.S.**[c], **Soo Min Koo, B.A.**[b], **Andrew Park, B.S.**[b], **Ghedem Solomon, M.S.**[b], **Melin Vranesic, M.D.**[b], **Inga Antonsdottir, RN, BSN**[a], **Caroline L. Speck, B.A.**[a], **Kelly Rootes-Murdy, M.S.**[a], **Alexandria Lerner, B.S.**[a], **Steven P. Rowe, M.D., Ph.D.**[b], **Yuchuan Wang, Ph.D.**[b], **Wojciech G. Lesniak, Ph.D.**[b], **Il Minn, Ph.D.**[b], **Arnold Bakker, Ph.D.**[a], **Gwenn S. Smith, Ph.D.**[a,b], **Robert F. Dannals, Ph.D.**[b], **Hiroto Kuwabara, M.D., Ph.D.**[b], **Andrew Horti, Ph.D.**[b], **Dean F. Wong, M.D., Ph.D.**[a,b,d,e], and **Martin G. Pomper, M.D., Ph.D.**[a,b]

[a]Department of Psychiatry and Behavioral Sciences, Johns Hopkins Medical Institutions, Baltimore, MD, USA

[b]Russell H. Morgan Department of Radiology and Radiological Science, Johns Hopkins Medical Institutions, Baltimore, MD, USA

[c]Department of Biomedical Engineering, Johns Hopkins Medical Institutions, Baltimore, MD, USA

[d]Department of Neuroscience, Johns Hopkins Medical Institutions, Baltimore, MD, USA

[e]Department of Neurology, Johns Hopkins Medical Institutions, Baltimore, MD, USA

Abstract

Altered function of the alpha7 nicotinic acetylcholine receptor (α7-nAChR) is implicated in several neuropsychiatric diseases. Nevertheless, studies of the human cerebral α7-nAChR even in healthy aging are limited in number and to postmortem tissue.

Methods—The distribution of the cerebral α7-nAChR was estimated in nine brain regions in 25 healthy volunteers (ages 21–86 years; median 57 years, interquartile range 52 years) using [^{18}F]ASEM with positron emission tomography (PET) imaging. Regional total distribution volume (V_T) measurements were calculated using the Logan method from each subject's 90 min dynamic PET data and their metabolite-corrected plasma input function. Spearman's rank or Pearson's correlation analysis was used depending on the normality of the data. Correlation between age and regional 1) volume relative to intracranial volume (volume ratio) and 2) [^{18}F]ASEM V_T was tested. Correlation between regional volume ratio and [^{18}F]ASEM V_T was

Corresponding Author: Martin G. Pomper, M.D., Ph.D., CRB II, Room 492, 1550 Orleans Street, Baltimore, MD 21231, Tel: 410-955-2789; Fax: 443-817-0990; mpomper@jhmi.edu.

*Equal contribution.

The authors declare no conflicts of interest, including relevant financial interests, activities, relationships, and affiliations.

also evaluated. Finally, the relationship between [^{18}F]ASEM V_T and neuropsychological measures was investigated in a subpopulation of 15 elderly healthy participants (those 50 years of age and older). Bonferroni correction for multiple comparisons was applied to statistical analyses.

Results—A negative correlation between tissue volume ratio and age was observed in six of the nine brain regions including striatum and five cortical (temporal, occipital, cingulate, frontal, or parietal) regions. A positive correlation between [^{18}F]ASEM V_T and age was observed in all nine brain regions of interest (ROIs). There was no correlation between [^{18}F]ASEM V_T and volume ratio in any ROI after controlling for age. Regional [^{18}F]ASEM V_T and neuropsychological performance on each of eight representative subtests were not correlated among the well-performing subpopulation of elderly healthy participants.

Conclusions—Our results suggest an increase in cerebral α7-nAChR distribution over the course of healthy aging that should be tested in future longitudinal studies. The preservation of the α7-nAChR in the aging human brain supports the development of therapeutic agents that target this receptor for use in the elderly. Further study of the relationship between α7-nAChR availability and cognitive impairment over aging is needed.

Keywords

[^{18}F]ASEM; healthy aging; PET imaging; alpha7 nicotinic acetylcholine receptor

1. Text

1.1. Introduction

The alpha7 nicotinic acetylcholine receptor (α7-nAChR) is expressed on neurons and has functional roles in synaptic transmission, neurotransmitter release, intracellular signaling, and synaptic plasticity that collectively mediate cognitive function (Wallace and Porter, 2011). Human post-mortem studies support altered distribution of the cerebral α7-nAChR in neuropsychiatric illness, including studies of schizophrenia (Freedman et al., 1995; Marutle et al., 2001) and Alzheimer's disease (Guan et al., 2000). Since there is evidence implicating the α7-nAChR in various disease processes, the utility of new therapies targeting the α7-nAChR is being evaluated in patient populations with cognitive or affective symptoms (D'Hoedt and Bertrand, 2009; Hurst et al., 2013; Mazurov et al., 2012; Mazurov et al., 2011; Olincy et al., 2006; Shytle et al., 2002; Taly and Charon, 2012). Nevertheless, our understanding of the availability of the α7-nAChR even in healthy aging is incomplete since studies of human brain tissue that focus on this receptor subtype are limited in number and to a narrow selection of examined regions (Perry et al., 2001). New techniques designed to image the α7-nAChR *in vivo* promise to help elucidate changes in the distribution of the cerebral α7-nAChR in healthy aging and disease (Horti, 2015; Horti et al., 2014).

A radioligand for imaging the α7-nAChR, [^{18}F]ASEM, was developed by our group (Horti, 2015) and has shown promising pharmacokinetic characteristics in early human neuroimaging studies using positron emission tomography (PET) (Hillmer et al., 2017; Wong et al., 2014). [^{18}F]ASEM enters the brain rapidly and within 15–30 min after intravenous (IV) bolus radiotracer injection the standardized uptake values peak around 3.0–4.5 before gradual decline in all regions. Two recent studies using this radiotracer in human

neuroimaging support the use of graphical analysis (plasma reference graphical analysis [PRGA], multilinear analysis method [MA1]) to derive the primary binding outcome, regional total distribution volume (V_T), using data from at least 90 min of dynamic imaging (Hillmer et al., 2017; Wong et al., 2014). The test-retest variability of [^{18}F]ASEM human PET data was 10.8 ± 5.1% and 11.7 ± 9.8% across the brain regions tested in these two independent studies of healthy controls.

Here, we aimed to use [^{18}F]ASEM PET-based neuroimaging in a new group of healthy individuals to investigate the availability of the α7-nAChR within the context of healthy aging. We focused on the binding of [^{18}F]ASEM in nine regions, including those suspected to have lower (thalamus, frontal cortex) or unchanged (hippocampus, striatum) availability of the α7-nAChR in the aged brain based on limited results using α-bungarotoxin or assay of mRNA in human postmortem tissue (Court et al., 1997; Hellstrom-Lindahl and Court, 2000; Nordberg and Winblad, 1986; Utsugisawa et al., 1999). Since decline in cholinergic signaling is seen across the lifespan and may be linked to compensatory re-distribution of the α7-nAChR or to cognitive deficits in elderly individuals, we also assessed the relationship between regional [^{18}F]ASEM V_T and 1. regional brain volume as well as 2. cognitive performance, the latter among the subset of participants who were 50 years of age or older.

2. Materials and Methods

2.1. Human Subjects

A Johns Hopkins Institutional Review Board approved this study and all participants provided written informed consent. Use of [^{18}F]ASEM is conducted under FDA exploratory IND 118496. Healthy adult (over age 18 years) participants were recruited through local advertising. Each subject completed a careful clinical interview and physical assessment with screening blood work, electrocardiogram (EKG), and urine toxicology. Eligibility criteria included stable health, with no clinical abnormality on a screening health assessment and the structural magnetic resonance imaging (MRI). Exclusion criteria included nicotine use, any current or past psychiatric or neurological illness (including history of head injury with loss of consciousness), history of recreational substance abuse including marijuana (assessed by self-report and urine toxicology), prescribed medication known to affect acetylcholine signaling (including but not limited to anticholinergic and certain $5HT_3$ anti-emetic medications), any current psychotropic medication use, contraindication to MRI (i.e. implanted metal, claustrophobia), or contraindication to PET imaging with arterial line placement (i.e. clotting factor deficiency, pregnancy/breast feeding, prior radiation exposure). Participants completed the Mini Mental State Examination (MMSE) (Folstein et al., 1975) to assess global cognitive performance. Older participants (age 50 years and older) in this study were also assessed using a battery of neuropsychological tests. We chose to focus on eight representative subtests from this comprehensive battery to characterize performance of these elderly participants across the neurocognitive domains of attention [Digit Span Forwards from Wechsler Adult Intelligence Scale Third Edition (Wechsler, 1997); Delis-Kaplan Executive Functioning System (DKEFS) (Delis et al., 2001) Number Sequencing Time], working memory [DKEFS Number-Letter Sequencing Time], language

[DKEFS Category Fluency]; executive function [DKEFS Letter Fluency], visuospatial ability [Clock Drawing Test (Freedman, 1994)], and verbal learning and memory [California Verbal Learning Test (CVLT) (Delis et al., 1987) Total Recall from Trials 1–5; CVLT Long Delay Free Recall].

2.2. DNA Extraction and Genotyping

A blood sample was collected from those participants age 50 years and older for DNA extraction (PureGene® Blood Core Kit C, Qiagen, Valencia, CA) according to manufacturer's instructions. Genotyping of the two single nucleotide polymorphisms (SNPs) that determine the three possible alleles of the gene for apolipoprotein E, *APOE*, was completed using TaqMan genotyping assays (rs429358: cat# 4351379, rs7412: cat# 4351379, Applied Biosytems, Foster City, CA) on a CFX96 Touch™ Real-Time PCR Detection System (Bio-Rad, Hercules, CA). Analyses of the six different *APOE* genotypes: ε2/ε2, ε3/ε3, ε4/ε4, ε2/ε3, ε2/ε4, and ε3/ε4 were completed using the CFX Manager™ Software (Bio-Rad, Hercules, CA). Individuals with at least one ε4 allele were categorized as APOE ε4 carriers.

2.3. In Vivo Brain Imaging

2.3.1. Radiotracer synthesis and PET acquisition—[^{18}F]ASEM was synthesized as previously described by one-step microwave radiosynthesis via the corresponding nitro-precursor (Gao et al., 2013), and met all U.S. Pharmacopeia Convention Chapter <823> acceptance testing criteria. Radiochemical purity at end of synthesis was > 98% with high specific radioactivity (2,306 ± 2,164 GBq/μmol) at the time of IV bolus radiotracer injection and onset of the dynamic list mode PET acquisition. The average injected dose of radioactivity was 510.1 ± 41.0 MBq with injected mass of 0.19 ± 0.17 μg.

2.3.2. PET acquisition—A thermoplastic mask was fitted to each subject's face for immobilization and positioning of the head during scanning. PET continuous listmode data were acquired using a High Resolution Research Tomograph scanner (HRRT, Siemens Healthcare, Knoxville,TN), an LSO-based, dedicated brain PET scanner with < 2.5 mm reconstructed image resolution (Sossi et al., 2005). Four participants (two females with ages 26 and 82 years, and two males with ages 25 and 67 years) underwent data collection for 120 min. This longer scan time was used to validate further the use of a 90 min emission scan. Ninety min of continuous listmode data were acquired from each subsequent participant. One hundred twenty min of listmode data were binned into 36 frames (four 15 s, four 30 s, three 1 min, two 2 min, five 4 min, and eighteen 5 min frames). Ninety min of listmode data were binned using the same frame protocol with six less 5 min frames (total of 30 frames). The data were then reconstructed using the iterative ordinary-Poisson ordered-subset expectation-maximization algorithm (6 iteration and 16 subsets, 2 mm post-smoothing), with correction for radioactive decay, dead time, attenuation, scatter and randoms (Rahmim et al., 2005). The attenuation maps were generated from 6 min transmission scans performed with a ^{137}Cs point source prior to the emission scans. The reconstructed image volume spanned 31 cm × 31 cm transaxially and 25 cm axially. The image matrix consisted of 256 × 256 × 207 voxels and a voxel size of 1.22 × 1.22 × 1.22 mm^3.

2.3.3. Plasma sampling—All participants underwent radial arterial line placement prior to radiotracer injection. Measurement of the arterial plasma input function was conducted through collection of 35 – 50 blood samples (1 mL) that were obtained at the following intervals after bolus radiotracer injection (p.i.): as fast as possible for the initial 1.5 min p.i., every 30 seconds between 1.5 – 3 min p.i., once at 5 min p.i., and then every five min for the duration of the 90 or 120 min continuous emission scan. The fraction of parent radioligand in plasma was determined by high performance liquid chromatography (HPLC) analysis from collection of 3–6 mL blood samples before radiotracer injection (background) and at 5, 10, 20, 30, 45, 60, 75, and 90 min p.i. Scans lasting 120 min had additional blood sampling for metabolite measurements at 105 and 120 min p.i.

Briefly, the modified column-switching HPLC method (Hilton et al., 2000) used an Agilent Technologies system containing a 1260 Infinity quaternary pump, a 1260 Infinity column compartment module, a 1260 Infinity UV detector, and a Bioscan radiation detector that was controlled by OpenLab CDS EZChrom (A.01.04) software. Each plasma sample (1–2 mL) was loaded onto a 4 mL Rheodyne injector loop and was initially directed to the capture column (packed with Phenomenex Strata-X 33μm polymeric reversed phase sorbent) and detectors using 1% acetonitrile and 99% water mobile phase at 2 mL/min to detect polar metabolites. After 2 min of elution, an analytical mobile phase composed of 40% acetonitrile and 60% aqueous triethylamine at a concentration of 0.1 M and pH = 7.1 (adjusted with phosphoric acid) was applied to elute trapped non-polar metabolites and parent radiotracer onto an analytical column (Waters, reverse phase XBridge BEH C18 5 μM 4.6 × 250 mm) at 2 mL/min.

2.3.4. Measurement of Plasma Free Fraction (f_P)—Plasma Free Fraction (f_P) was measured using rapid equilibrium dialysis (RED). Plasma samples were isolated by centrifugation from one blood sample obtained from each participant before radiotracer injection. A 300 μL sample of plasma was spiked with 3 μCi of [^{18}F]ASEM and added into the sample chamber of Single-Use RED Plate with Inserts (Thermo Scientific, Rockford, IL, USA) with an 8 K molecular-weight cutoff. 500 μL of PBS was added to the buffer chamber and the plate was incubated on an Incubating Microplate Shaker (Fisher Scientific, Waltham, MA, USA) at 37°C for 4 h. 100 μL of plasma and 100 μL of PBS were transferred to a clean tube. All samples were measured in triplicate. The radioactivity was measured using a 2480 WIZARD^2 Gamma Counter (Perkin Elmer, Waltham, MA, USA) to obtain the radioactivity in the plasma (C_P) and buffer (C_U). The free, unbound fraction (f_P) was calculated as: $f_P = C_U / C_P \times 100$ (%).

2.3.5. MRI acquisition—MR structural T1-weighted imaging was acquired on a Siemens MAGNETOM Prisma or on a Siemens MAGNETOM Trio 3 Tesla scanner (Malvern, PA, USA) with a Trio head matrix 12-channel head coil or Prisma head/neck 20-channel head coil, to obtain a 0.8 × 0.8 × 0.8 mm^3 3-dimensional (3D) Magnetization-Prepared Rapid Gradient-Echo (MP-RAGE) sequence.

2.4. Data Analysis and Statistics

2.4.1. Image processing—The software package PMOD (v3.7, PMOD Technologies Ltd, Zurich, Switzerland) was used in the initial PET image processing and kinetic analysis. Inter-frame motion correction was applied post-reconstruction using the motion correction function in PMOD. First, a static reference frame was generated by averaging the frames corresponding to the 30–60 minutes p.i. Second, the motion correction was accomplished by rigid matching of the dynamic data to the reference image frame by frame. PET-MRI co-registration was completed as previously described (Coughlin et al., 2015). Cortical reconstruction and volumetric segmentation of T1-weighted MR images were performed with the FreeSurfer image analysis suite (http://surfer.nmr.mgh.harvard.edu/). Nine regions of interest (ROIs) were selected for this study: thalamus, striatum, hippocampus, cerebellar cortex, temporal cortex, occipital cortex, cingulate cortex, frontal cortex and parietal cortex. Total intracranial volume (ICV) was also defined using FreeSurfer, for use in analyses exploring the correlation between age and ROI volume normalized to ICV, herein referred to as regional volume ratio. Correlation between regional volume ratio and binding of [^{18}F]ASEM was also tested. PET time-activity curves (TACs) were generated for all subjects using the ROI definitions.

2.4.2. Calculation of regional total distribution volume (V_T)—The primary PET-based regional binding outcome was total distribution volume, V_T, defined as the ratio of the concentration of the radioligand in brain tissue to that in plasma at equilibrium (Innis et al., 2007). The kinetics of [^{18}F]ASEM can be modeled using graphical analysis (Hillmer et al., 2017; Wong et al., 2014). Here, V_T within each ROI was estimated using Logan graphical analysis (Logan et al., 1990) with fixed t* = 45 min, which was chosen for its computational simplicity and independence from assumed compartmental characteristics of the data. Regional V_T values generated using Logan analysis with metabolite-corrected arterial input function from 120 min dynamic scans among four participants were compared to V_T values obtained with data shortening down to 90 min in order to validate further the proposed use of 90 min of continuous PET data. Since the 1TCM yields equal (Wong et al., 2014) or improved (Hillmer et al., 2017) model suitability compared to two-tissue compartmental modeling (2TCM), regional V_T values from the Logan method were compared to those generated using one-tissue compartmental modeling (1TCM) using 90 min data for all 25 individuals. Compartmental modeling used a fixed blood volume of 5%. Plasma free fraction (f_P) was measured for 18 of the 25 subjects, with mean ± standard deviation (SD) = 0.05 ± 0.01. Regional V_T corrected for f_P (V_T/f_P) was calculated as a secondary outcome measure for those individuals with measured f_P.

2.5. Statistical Analysis

Statistical analyses were performed using SPSS Statistics (Version 23.0, IBM Corp., Armonk, NY, USA). Data were checked for outliers, and descriptive statistics were obtained. Normality of the data was assessed using the Shapiro-Wilk test. The relationships between 1) regional [^{18}F]ASEM V_T values and age (as well as other descriptive variables) and 2) ROI volume ratios and age were tested using Spearman's rank-order correlation analysis since age was found to not be normally distributed across the study population. These analyses were repeated for the secondary binding outcome, regional V_T/f_P.

The threshold for significance for all statistical tests involving regional V_T and regional volume measures accounted for the nine ROIs using a Bonferroni adjusted alpha level of 0.0056 per test (approximately =0.05/9). The threshold for significance in all statistical tests involving the eight representative neuropsychological tests was set as $P < 0.0063$ (approximately = 0.05/8). Data were expressed as mean ± SD unless otherwise noted.

3. Results

3.1. Human Subject Participation

Twenty-five healthy participants, ranging in ages from 21–86 (median 57; interquartile range 52) years participated in [^{18}F]ASEM PET neuroimaging (Table 1). Participants had 13–23 years of education. Four of the 25 participants (ages 27.75 ± 5.12 years, range 21–33 years) did not complete the MMSE on the morning of the PET due to late addition of this test variable. MMSE scores among 21 participants ranged from 27–30 out of 30 possible points (29.38 ± 0.92). There was no correlation between MMSE and age. All 15 older (defined as age 50 years or older) participants completed the neuropsychological assessment (Table 2). Increasing age was not associated with poorer cognitive performance on any of the eight representative tests (Supplemental Table 1). Three of the 15 elderly individuals were found to be APOE ε4 carriers.

3.2. Regional Volumes

ROI volumes as well as ICV are presented in Table 3. Spearman's rank-order correlation analyses revealed negative correlation between regional volume ratio and age in striatum, temporal cortex, occipital cortex, cingulate cortex, frontal cortex, and parietal cortex (Table 3, Figure 1).

3.3. [^{18}F]ASEM PET imaging

Regional V_T values generated using Logan analysis with metabolite-corrected arterial input function from 90 min continuous scans were within 5% of the V_T values obtained using 120 min of continuous [^{18}F]ASEM data (Supplemental Figure 1, Supplemental Table 2). Using 90 min data, regional V_T values from the Logan method were comparable to V_T values estimated using the 1TCM (Table 4). Furthermore, regional V_T values from the Logan method highly correlated with those from using the 1TCM (Spearman's rho = 0.945, $P < 0.001$) (Supplemental Figure 2).

Spearman's rank-order correlation analyses revealed no correlation between K_1 and age in all nine regions of interest. Regional V_T values generated using Logan analysis with metabolite-corrected arterial input function from 90 min scan duration were used in all other correlation analyses hereafter, unless otherwise stated.

Spearman's rank-order correlation analyses revealed positive correlation between [^{18}F]ASEM regional V_T values and age in all nine ROIs (Table 4, Figure 2). Secondary analyses revealed positive correlation between V_T/f_P and age in striatum and parietal cortex (Supplemental Table 3), and f_P did not correlate with age. There was no correlation between [^{18}F]ASEM V_T in any of the ROIs and sex, race, body mass index, years of education, or

MMSE score. There was no correlation between [^{18}F]ASEM V_T and volume ratio in any ROI after controlling for age (Supplemental Table 4). Finally, post hoc analyses revealed positive correlation between [^{18}F]ASEM V_T estimates from the 1TCM and age in six of the nine ROIs (Supplemental Table 5).

Among the 15 individuals age 50 years and older, there was no significant correlation found between [^{18}F]ASEM V_T in any ROI and performance on any of the eight representative cognitive measures after Bonferroni correction. However, without correction for multiplicity, a negative correlation ($P < 0.05$) between the DKEFS Number Sequencing Time, a test of attention, and [^{18}F]ASEM V_T in occipital cortex (*rho* = −0.534, $P = 0.040$) was observed, reflecting a trend of poorer performance in those with lower binding in this region (Supplemental Figure 3).

4. Discussion

The relationship between cognitive decline in healthy aging and cholinergic dysfunction is likely related to complex underlying factors that may include loss of cholinergic projections, deficits in acetylcholine signaling with secondary effects on other neurotransmitter release, or changed distribution of nicotinic receptor subtypes (Court et al., 2000). Converging evidence from pharmacological studies and animal models suggests the important role of the α7-nAChR in cognitive function (Levin, 2012). The ability to estimate the distribution of the α7-nAChR *in vivo* using [^{18}F]ASEM with PET imaging may help elucidate the hypothesized link between cerebral α7-nAChR availability and cognitive decline, even over the healthy human lifespan (Horti, 2015; Horti et al., 2014).

In the present study, we assessed the relationship between the availability of the α7-nAChR and healthy aging. Using non-parametric (Spearman's rank) correlation analysis, a positive correlation between [^{18}F]ASEM V_T and age was observed in all nine ROIs, which included cortical and subcortical regions. Consistent with previously reported regional decreases in brain volume over normal aging (De Leon et al., 1997; Driscoll et al., 2009; Tisserand et al., 2004), we observed a negative correlation between the tissue volume ratio and age in several of these ROIs, namely striatum, temporal cortex, occipital cortex, cingulate cortex, frontal cortex, and parietal cortex. There was no correlation between [^{18}F]ASEM V_T and volume ratio in any ROI after controlling for age. While this study is limited by small sample size, our results support the promising utility of [^{18}F]ASEM neuroimaging to examine the relationship between the distribution of the α7-nAChR, onset of regional brain atrophy, and related clinical changes over the course of healthy aging. Furthermore, these results suggest a link between higher cerebral availability of the α7-nAChR with aging that may prove important to our understanding of cholinergic signaling over the lifespan. Specifically, these results suggest an increase in the cerebral α7-nAChR, perhaps as a compensatory response to lower acetylcholine signaling, over the course of healthy aging that should be tested in animal models and future longitudinal studies. The preservation of the α7-nAChR over normal aging supports the development of therapeutic agents that target this receptor for treatment of cognitive dysfunction in the elderly.

This study benefits from several methodological strengths including a larger sample size of [^{18}F]ASEM neuroimaging data from healthy individuals compared to two other recent studies (Hillmer et al., 2017; Wong et al., 2014). [^{18}F]ASEM neuroimaging data from this new group of 25 healthy individuals spanning ages 21–86 years showed that use of the Logan graphical method with metabolite-corrected arterial input function, like other methods of graphical analysis (Hillmer et al., 2017; Wong et al., 2014), yields regional V_T estimates that are similar to those from the preferred compartmental tissue model, the 1TCM (Hillmer et al., 2017), using 90 min of continuous dynamic emission data. One-hundred twenty min of emission data were acquired from four (two young and two elderly) of our 25 healthy participants and data shortening showed that V_T estimates from a 90 min scan duration were within 5% of the values estimated from a 120 min scan duration for all ROIs. The methodological design also included careful assessment of neuropsychological performance in those individuals who were 50 years old or older in order to probe the relationship between distribution of [^{18}F]ASEM binding and cognitive performance in late aging. This small subpopulation of 15 elderly controls showed no correlation between performance on the selected neuropsychological subtests and increasing age. Similarly, there were no significant correlations found between regional [^{18}F]ASEM V_T values and cognitive measures among this well-performing population of healthy participants. Nevertheless, the observed trend of a negative correlation between performance on the DKEFS Number Sequencing, a test of attention, and [^{18}F]ASEM V_T in occipital cortex should be tested further in larger studies of aging individuals with more varied neuropsychological performance given the hypothesized key role of the α7-nAChR in modulating tasks of sustained attention (Young et al., 2004).

There are some important methodological and biological factors that should be considered and further investigated in future [^{18}F]ASEM PET imaging studies in aging and disease. First, we defined regional V_T as our primary binding outcome. Since only free radioligand enters brain, we also measured f_P, and calculated regional V_T/f_P as a secondary outcome measure. The values obtained for f_P were 5 ± 1% and therefore very similar to those reported in six healthy participants (7.7 ± 1.3%) by Hillmer et al. However, the correlation between [^{18}F]ASEM binding and age was only observed in striatum and parietal cortex using V_T/f_P as the binding outcome. Since f_P is an independent measurement and may introduce further noise from plasma data, it is possible that [^{18}F]ASEM lacks sensitivity to detect changes in V_T/f_P in all affected ROIs over aging, especially in the setting of small sample size. On the other hand, the limited number of postmortem studies to-date do not report evidence of higher availability of the α7-nAChR in elderly cases (Perry et al., 2001). Since amyloid burden in the brain may also be associated with upregulated cerebral expression of the α7-nAChR (Ikonomovic et al., 2009; Nishiyama et al., 2015), the effect of this potential synergistic relationship should be examined in future *in vivo* or *in vitro* studies. Since there were only three individuals found to be APOE4 carriers in this population, we could not sufficiently test for this effect that could be a focus of future studies. Second, it is important to note that [^{18}F]ASEM PET signal is only an indirect measure of the α7- nAChR in the living brain. Our results support further *in vitro* experiments of the α7-nAChR directly, in carefully selected postmortem tissue from individuals of all ages.

Conclusions

By demonstrating a positive correlation between [^{18}F]ASEM binding and age in several brain regions of healthy individuals, we support future use of [^{18}F]ASEM PET to examine the relationship between altered distribution of the α7-nAChR and clinical changes even over healthy aging. Since there is interest in targeting this receptor subtype to prevent or ameliorate cognitive deficits, human studies using [^{18}F]ASEM in individuals with more robust impairment in cognitive performance will inform further the lack of observed relationship between [^{18}F]ASEM V_T and performance on neuropsychological tests among elderly participants reported here. [^{18}F]ASEM PET continues to demonstrate promise as a research tool for testing the relationship between altered availability of the cerebral α7-nAChR in clinical populations, toward guiding therapies targeted to this receptor subtype.

Supplementary Material

Refer to Web version on PubMed Central for supplementary material.

Acknowledgments

This work was supported by the Henry N. Wagner, Jr. Endowment (MGP), the Alexander Wilson Schweizer Fellowship (JC), and the National Institutes of Health [R01 MH107197 (DFW and AH), AG038893 (GSS), AG041633 (GSS), Shared Instrument Grants S10RR023623 (DFW), S10RR017219 (DFW)]. The authors would also like to thank the Johns Hopkins PET Center for expert provision of [^{18}F]ASEM, with special thanks to Alimamy Kargbo for PET metabolite analyses. We thank Lorena Gapasin, BSN, MS who assisted in regulatory matters and Josh Roberts, PhD and Kelly Kitzmiller, BS who assisted in recruitment and characterization of some of the younger healthy subjects. We also give special thanks to Yukiko Lema for assistance in the figure design.

References

Coughlin JM, Wang Y, Munro CA, Ma S, Yue C, Chen S, Airan R, Kim PK, Adams AV, Garcia C, Higgs C, Sair HI, Sawa A, Smith G, Lyketsos CG, Caffo B, Kassiou M, Guilarte TR, Pomper MG. Neuroinflammation and brain atrophy in former NFL players: An in vivo multimodal imaging pilot study. Neurobiol Dis. 2015; 74:58–65. [PubMed: 25447235]

Court JA, Lloyd S, Johnson M, Griffiths M, Birdsall NJ, Piggott MA, Oakley AE, Ince PG, Perry EK, Perry RH. Nicotinic and muscarinic cholinergic receptor binding in the human hippocampal formation during development and aging. Brain Res Dev Brain Res. 1997; 101:93–105. [PubMed: 9263584]

Court JA, Martin-Ruiz C, Graham A, Perry E. Nicotinic receptors in human brain: topography and pathology. J Chem Neuroanat. 2000; 20:281–298. [PubMed: 11207426]

D'Hoedt D, Bertrand D. Nicotinic acetylcholine receptors: an overview on drug discovery. Expert Opin Ther Targets. 2009; 13:395–411. [PubMed: 19335063]

De Leon MJ, George AE, Golomb J, Tarshish C, Convit A, Kluger A, De Santi S, McRae T, Ferris SH, Reisberg B, Ince C, Rusinek H, Bobinski M, Quinn B, Miller DC, Wisniewski HM. Frequency of hippocampal formation atrophy in normal aging and Alzheimer's disease. Neurobiol Aging. 1997; 18:1–11. [PubMed: 8983027]

Delis, DC., Kaplan, E., Kramer, J. Delis–Kaplan Executive Function System. Psychological Corporation; San Antonio, TX: 2001.

Delis, DC., Kramer, JH., Kaplan, E., Ober, BA. CVLT, California Verbal Learning Test: Adult Version: Manual. Psychological Corporation; San Antonio, TX: 1987.

Driscoll I, Davatzikos C, An Y, Wu X, Shen D, Kraut M, Resnick SM. Longitudinal pattern of regional brain volume change differentiates normal aging from MCI. Neurology. 2009; 72:1906–1913. [PubMed: 19487648]

Folstein MF, Folstein SE, McHugh PR. “Mini-mental state”. A practical method for grading the cognitive state of patients for the clinician. J Psychiatr Res. 1975; 12:189–198. [PubMed: 1202204]

Freedman, M. Clock drawing: A neuropsychological analysis. Oxford University Press; NY, New York: 1994.

Freedman R, Hall M, Adler LE, Leonard S. Evidence in postmortem brain tissue for decreased numbers of hippocampal nicotinic receptors in schizophrenia. Biol Psychiatry. 1995; 38:22–33. [PubMed: 7548469]

Gao Y, Kellar KJ, Yasuda RP, Tran T, Xiao Y, Dannals RF, Horti AG. Derivatives of dibenzothiophene for positron emission tomography imaging of alpha7-nicotinic acetylcholine receptors. J Med Chem. 2013; 56:7574–7589. [PubMed: 24050653]

Guan ZZ, Zhang X, Ravid R, Nordberg A. Decreased protein levels of nicotinic receptor subunits in the hippocampus and temporal cortex of patients with Alzheimer’s disease. J Neurochem. 2000; 74:237–243. [PubMed: 10617125]

Hellstrom-Lindahl E, Court JA. Nicotinic acetylcholine receptors during prenatal development and brain pathology in human aging. Behav Brain Res. 2000; 113:159–168. [PubMed: 10942042]

Hillmer AT, Li S, Zheng MQ, Scheunemann M, Lin SF, Nabulsi N, Holden D, Pracitto R, Labaree D, Ropchan J, Teodoro R, Deuther-Conrad W, Esterlis I, Cosgrove KP, Brust P, Carson RE, Huang Y. PET imaging of alpha7 nicotinic acetylcholine receptors: a comparative study of [18F]ASEM and [18F]DBT-10 in nonhuman primates, and further evaluation of [18F]ASEM in humans. Eur J Nucl Med Mol Imaging. 2017

Hilton J, Yokoi F, Dannals RF, Ravert HT, Szabo Z, Wong DF. Column-switching HPLC for the analysis of plasma in PET imaging studies. Nucl Med Biol. 2000; 27:627–630. [PubMed: 11056380]

Horti AG. Development of [(18)F]ASEM, a specific radiotracer for quantification of the alpha7-nAChR with positron-emission tomography. Biochem Pharmacol. 2015; 97:566–575. [PubMed: 26232729]

Horti AG, Gao Y, Kuwabara H, Wang Y, Abazyan S, Yasuda RP, Tran T, Xiao Y, Sahibzada N, Holt DP, Kellar KJ, Pletnikov MV, Pomper MG, Wong DF, Dannals RF. 18F-ASEM, a radiolabeled antagonist for imaging the alpha7−nicotinic acetylcholine receptor with PET. J Nucl Med. 2014; 55:672–677. [PubMed: 24556591]

Hurst R, Rollema H, Bertrand D. Nicotinic acetylcholine receptors: from basic science to therapeutics. Pharmacol Ther. 2013; 137:22–54. [PubMed: 22925690]

Ikonomovic MD, Wecker L, Abrahamson EE, Wuu J, Counts SE, Ginsberg SD, Mufson EJ, Dekosky ST. Cortical alpha7 nicotinic acetylcholine receptor and beta-amyloid levels in early Alzheimer disease. Arch Neurol. 2009; 66:646–651. [PubMed: 19433665]

Innis RB, Cunningham VJ, Delforge J, Fujita M, Gjedde A, Gunn RN, Holden J, Houle S, Huang SC, Ichise M, Iida H, Ito H, Kimura Y, Koeppe RA, Knudsen GM, Knuuti J, Lammertsma AA, Laruelle M, Logan J, Maguire RP, Mintun MA, Morris ED, Parsey R, Price JC, Slifstein M, Sossi V, Suhara T, Votaw JR, Wong DF, Carson RE. Consensus nomenclature for in vivo imaging of reversibly binding radioligands. J Cereb Blood Flow Metab. 2007; 27:1533–1539. [PubMed: 17519979]

Levin ED. α7-nicotinic receptors and cognition. Curr Drug Targets. 2012; 13:602–606. [PubMed: 22300026]

Logan J, Fowler JS, Volkow ND, Wolf AP, Dewey SL, Schlyer DJ, MacGregor RR, Hitzemann R, Bendriem B, Gatley SJ, et al. Graphical analysis of reversible radioligand binding from time-activity measurements applied to [N-11C-methyl]-(-)-cocaine PET studies in human subjects. J Cereb Blood Flow Metab. 1990; 10:740–747. [PubMed: 2384545]

Marutle A, Zhang X, Court J, Piggott M, Johnson M, Perry R, Perry E, Nordberg A. Laminar distribution of nicotinic receptor subtypes in cortical regions in schizophrenia. J Chem Neuroanat. 2001; 22:115–126. [PubMed: 11470559]

Mazurov AA, Kombo DC, Hauser TA, Miao L, Dull G, Genus JF, Fedorov NB, Benson L, Sidach S, Xiao Y, Hammond PS, James JW, Miller CH, Yohannes D. Discovery of (2S,3R)-N-[2-(pyridin-3-ylmethyl)-1-azabicyclo[2.2.2]oct-3-yl]benzo[b]furan-2-car boxamide (TC-5619), a selective

alpha7 nicotinic acetylcholine receptor agonist, for the treatment of cognitive disorders. J Med Chem. 2012; 55:9793–9809. [PubMed: 23126648]

Mazurov AA, Speake JD, Yohannes D. Discovery and development of alpha7 nicotinic acetylcholine receptor modulators. J Med Chem. 2011; 54:7943–7961. [PubMed: 21919481]

Nishiyama S, Ohba H, Kanazawa M, Kakiuchi T, Tsukada H. Comparing alpha7 nicotinic acetylcholine receptor binding, amyloid-beta deposition, and mitochondria complex-I function in living brain: A PET study in aged monkeys. Synapse. 2015; 69:475–483. [PubMed: 26234533]

Nordberg, A., Winblad, B. Brain Nicotinic and Muscarinic Receptors in Normal Aging and Dementia. In: Fisher, A.Hanin, I., Lachman, C., editors. Alzheimer's and Parkinson's Disease: Strategies for Research and Development. Springer US; Boston, MA: 1986. p. 95-108.

Olincy A, Harris JG, Johnson LL, Pender V, Kongs S, Allensworth D, Ellis J, Zerbe GO, Leonard S, Stevens KE, Stevens JO, Martin L, Adler LE, Soti F, Kem WR, Freedman R. Proof-of-concept trial of an alpha7 nicotinic agonist in schizophrenia. Arch Gen Psychiatry. 2006; 63:630–638. [PubMed: 16754836]

Perry EK, Martin-Ruiz CM, Court JA. Nicotinic receptor subtypes in human brain related to aging and dementia. Alcohol. 2001; 24:63–68. [PubMed: 11522424]

Rahmim A, Cheng JC, Blinder S, Camborde ML, Sossi V. Statistical dynamic image reconstruction in state-of-the-art high-resolution PET. Phys Med Biol. 2005; 50:4887–4912. [PubMed: 16204879]

Shytle RD, Silver AA, Sheehan KH, Sheehan DV, Sanberg PR. Neuronal nicotinic receptor inhibition for treating mood disorders: preliminary controlled evidence with mecamylamine. Depress Anxiety. 2002; 16:89–92. [PubMed: 12415531]

Sossi, V., Jong, HWAMd, Barker, WC., Bloomfield, P., Burbar, Z., Camborde, ML., Comtat, C., Eriksson, LA., Houle, S., Keator, D., Knob, C., Krais, R., Lammertsma, AA., Rahmim, A., Sibomana, M., Teras, M., Thompson, CJ., Trebossen, R., Votaw, J., Walker, M., Wienhard, K., Wong, DF. The second generation HRRT – a multi-centre scanner performance investigation. IEEE Nuclear Science Symposium Conference Record, 2005; 2005. p. 2195-2199.

Taly A, Charon S. alpha7 nicotinic acetylcholine receptors: a therapeutic target in the structure era. Curr Drug Targets. 2012; 13:695–706. [PubMed: 22300037]

Tisserand DJ, van Boxtel MP, Pruessner JC, Hofman P, Evans AC, Jolles J. A voxel-based morphometric study to determine individual differences in gray matter density associated with age and cognitive change over time. Cereb Cortex. 2004; 14:966–973. [PubMed: 15115735]

Utsugisawa K, Nagane Y, Tohgi H, Yoshimura M, Ohba H, Genda Y. Changes with aging and ischemia in nicotinic acetylcholine receptor subunit alpha7 mRNA expression in postmortem human frontal cortex and putamen. Neurosci Lett. 1999; 270:145–148. [PubMed: 10462115]

Wallace TL, Porter RH. Targeting the nicotinic alpha7 acetylcholine receptor to enhance cognition in disease. Biochem Pharmacol. 2011; 82:891–903. [PubMed: 21741954]

Wechsler, D. Wechsler Adult Intelligence Scale Administration and Scoring Manual. Psychological Corporation; San Antonio, TX: 1997.

Wong DF, Kuwabara H, Pomper M, Holt DP, Brasic JR, George N, Frolov B, Willis W, Gao Y, Valentine H, Nandi A, Gapasin L, Dannals RF, Horti AG. Human brain imaging of alpha7 nAChR with [(18)F]ASEM: a new PET radiotracer for neuropsychiatry and determination of drug occupancy. Mol Imaging Biol. 2014; 16:730–738. [PubMed: 25145965]

Young JW, Finlayson K, Spratt C, Marston HM, Crawford N, Kelly JS, Sharkey J. Nicotine improves sustained attention in mice: evidence for involvement of the alpha7 nicotinic acetylcholine receptor. Neuropsychopharmacology. 2004; 29:891–900. [PubMed: 14970827]

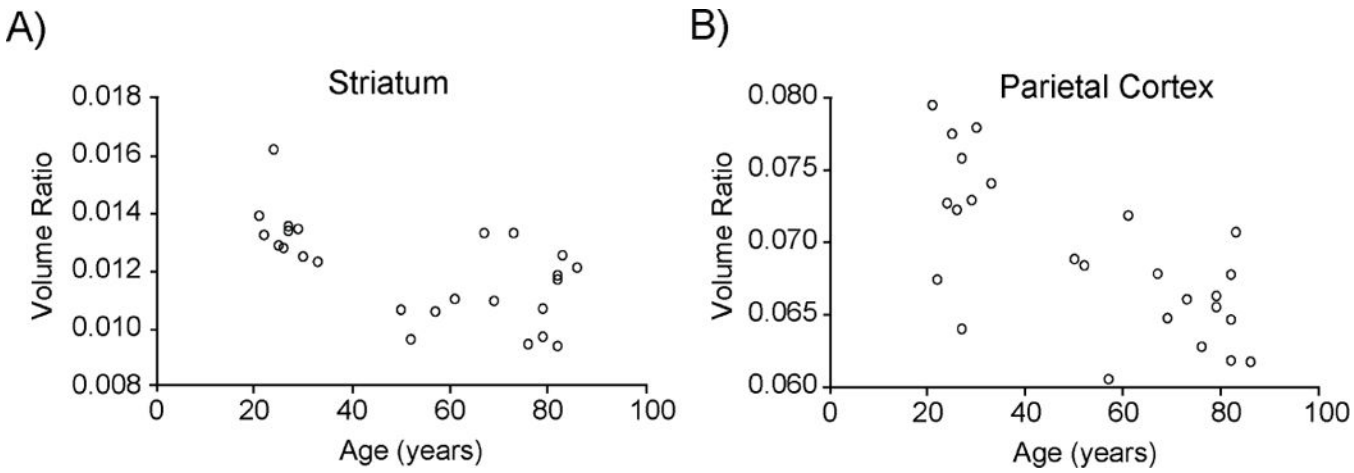

Figure 1. Scatter plots of regional volume relative to total intracranial volume (volume ratio) plotted against age

Spearman's rank-order correlation analyses revealed negative correlation between regional volume ratio (unitless) and age in six (striatum, temporal cortex, occipital cortex, cingulate cortex, frontal cortex, and parietal cortex) of the nine regions of interest. Individual data points are shown for two representative regions including A) Striatum (*rho* = −0.605, *P* = 0.001) and B) Parietal Cortex (*rho* = −0.627, *P* = 0.001). Significance was set at $P < 0.0056$ using Bonferroni correction for the nine regions tested.

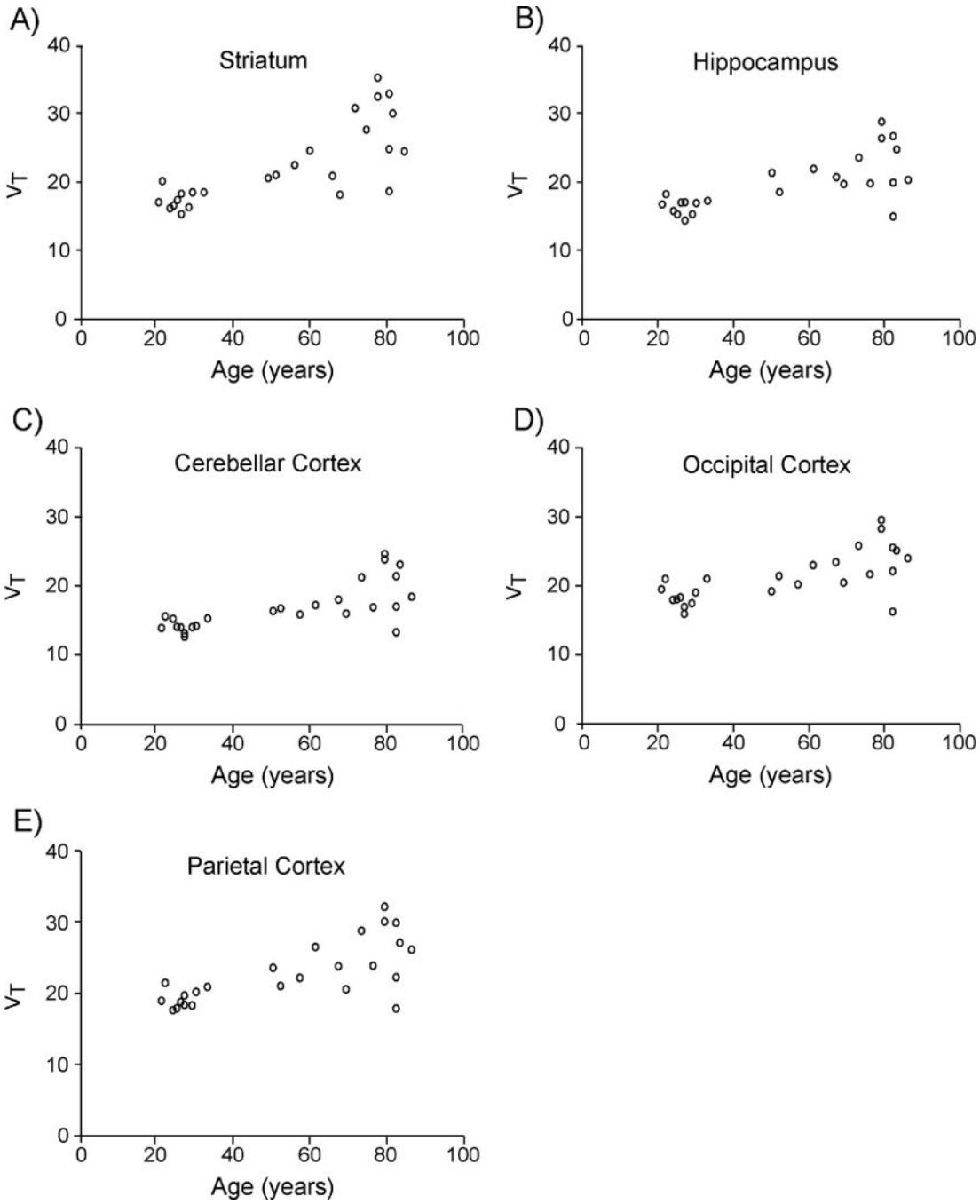

Figure 2. Scatter plots of regional [^{18}F]ASEM total distribution volume values (V_T) plotted against age

Regional V_T was estimated using metabolite-corrected arterial input function and Logan analysis (t* = 45 minutes) from 90 minute [^{18}F]ASEM data. Individual data points are shown for five representative regions including A) Striatum, B) Hippocampus, C) Cerebellar Cortex, D) Occipital Cortex and E) Parietal Cortex that were selected from the nine regions studied. Using Spearman's rank-order correlation analysis, all regions of interest in this study showed positive correlation between age and regional [^{18}F]ASEM V_T ($P < 0.0056$,

which marks significance after applying Bonferroni correction for the nine regions tested). V_T is in units of mL cm^{-3}.

Table 1

Clinical and demographic characteristics of 25 healthy human participants.

Age (years)	**53.68 ± 24.59**[a]
Sex (Male/Female)	15/10
Race (Caucasian/African-American)	18/7
Body mass index	24.61 ± 3.32
Education (years)	16.96 ± 2.37

[a] Results are presented as Mean ± Standard Deviation unless otherwise indicated.

Table 2

Neuropsychological performance in 15 elderly healthy control subjects.

Test	Elderly Controls[a,b]
Digit Span Forwards (Wechsler, 1997)	7.2 (0.8) 6–8
DKEFS (Delis et al., 2001) Number Sequencing Time (seconds)	36.6 (8.3) 19–47
DKEFS Number-Letter Sequencing Time (seconds)	97.7 (53.4) 41.4–272.0
DKEFS Category Fluency (Total number of words generated over 60 seconds)	39.2 (7.3) 29–57
DKEFS Letter Fluency (Total number of words generated over 60 seconds)	45.9 (11.1) 31–70
Clock Drawing Test (Freedman, 1994)	9.3 (1.1) 6–10
CVLT (Delis et al., 1987) Total number of words recalled – Sum of Trials 1–5	57.3 (10.5) 41–76
CVLT Long Delay Free Recall (Total number of words recalled – Single Trial)	12.4 (2.9) 7–16

[a]Elderly healthy controls were defined as those participants age 50 years and older and all completed the neuropsychological assessment that included these eight representative tests.

[b]Scores presented as Mean (Standard Deviation) and range. California Verbal Learning Test, CVLT; Delis-Kaplan Executive Functioning System, DKEFS).

Table 3

Regional volume measurements within the study population of 25 healthy individuals and correlation between age and regional volume ratio.

ROI	ROI Volume[a]	ROI Volume Ratio[a]	Rho (*P* value)[b]
Thalamus	15.25 ± 1.96	0.010 ± 0.001	−0.438 (0.029)
Striatum	18.05 ± 2.21	0.012 ± 0.002	−0.605 (0.001)*
Hippocampus	8.48 ± 0.80	0.006 ± 0.001	−0.242 (0.243)
Cerebellar CTX	104.83 ± 16.06	0.070 ± 0.009	−0.304 (0.140)
Temporal CTX	92.37 ± 13.20	0.061 ± 0.007	−0.737 (< 0.001)*
Occipital CTX	42.98 ± 5.17	0.029 ± 0.003	−0.562 (0.003)*
Cingulate CTX	19.44 ± 3.31	0.013 ± 0.001	−0.710 (< 0.001)*
Frontal CTX	165.69 ± 22.78	0.110 ± 0.009	−0.758 (< 0.001)*
Parietal CTX	103.95 ± 13.60	0.069 ± 0.005	−0.627 (0.001)*
Total ICV	1509.79 ±169.20	N/A	N/A

[a] Presented as Mean ± Standard Deviation. ROI volume is in units of cm^3. Volume relative to total intracranial volume (ICV) is defined as volume ratio and is unitless.

[b] Spearman's rank correlation analysis was applied to each test of correlation between age and ROI volume ratio. Cortex, CTX; Region of Interest, ROI.

* $P < 0.0056$, which marks significance after applying Bonferroni correction for the nine regions tested.

Table 4

K_1 and Total Distribution Volume (V_T) values estimated with the one-tissue compartmental model (1TCM), along with V_T values and Correlation between age and regional V_T estimated using Logan analysis (t* =45 minutes) for [^{18}F]ASEM PET imaging in humans(N=25).

ROI	1TCM		Logan	
	K_1[a] (mL cm^{-3} min^{-1})	V_T[a] (mL cm^{-3})	V_T[a] (mL cm^{-3})	Rho (*P* value)[b]
Thalamus	0.36 ± 0.06	21.44 ± 4.68	22.78 ± 5.15	0.591 (0.002)*
Striatum	0.35 ± 0.06	21.82 ± 5.96	22.60 ± 5.97	0.778 (< 0.001)*
Hippocampus	0.27 ± 0.05	17.92 ± 3.38	19.77 ± 3.97	0.666 (< 0.001)*
Cerebellar CTX	0.36 ± 0.06	16.17 ± 3.32	16.92 ± 3.44	0.718 (< 0.001)*
Temporal CTX	0.30 ± 0.05	21.20 ± 3.68	22.30 ± 3.94	0.621 (0.001)*
Occipital CTX	0.38 ± 0.07	20.34 ± 3.48	21.44 ± 3.66	0.652 (< 0.001)*
Cingulate CTX	0.35 ± 0.06	20.78 ± 3.31	21.85 ± 3.51	0.610 (0.001)*
Frontal CTX	0.36 ± 0.07	20.62 ± 4.16	21.45 ± 4.19	0.581 (0.002)*
Parietal CTX	0.36 ± 0.06	21.70 ± 4.18	22.78 ± 4.35	0.670 (< 0.001)*

[a] Presented as Mean ± Standard Deviation. Regional V_T values were generated using metabolite-corrected arterial input function and 90 minute dynamic data.

[b] Spearman's rank correlation analysis was applied to each test of correlation between age and regional V_T generated using Logan analysis. Cortex, CTX; Region of Interest, ROI.

* $P < 0.0056$, which marks significance after applying Bonferroni correction for the nine regions tested.